

This article was downloaded by:

On: 25 January 2011

Access details: *Access Details: Free Access*

Publisher *Taylor & Francis*

Informa Ltd Registered in England and Wales Registered Number: 1072954 Registered office: Mortimer House, 37-41 Mortimer Street, London W1T 3JH, UK



Separation Science and Technology

Publication details, including instructions for authors and subscription information:

<http://www.informaworld.com/smpp/title~content=t713708471>

Modeling of RO Flux Decline in Textile Wastewater Reclamation Plants Using Variable Fouling Index

Thirdpong Srisukphun^a; Chart Chiemchaisri^b; Kazuo Yamamoto^c

^a Department of Environmental Engineering, Faculty of Engineering, Kasetsart University, Bangkok, Thailand

^b Department of Environmental Engineering/National Center of Excellence for

Environmental and Hazardous Waste Management, Faculty of Engineering, Kasetsart University, Bangkok, Thailand

^c Environmental Science Center, The University of Tokyo, Hongo, Bunkyo-ku, Tokyo, Japan

To cite this Article Srisukphun, Thirdpong , Chiemchaisri, Chart and Yamamoto, Kazuo(2009) 'Modeling of RO Flux Decline in Textile Wastewater Reclamation Plants Using Variable Fouling Index', *Separation Science and Technology*, 44: 8, 1704 – 1721

To link to this Article: DOI: 10.1080/01496390902880057

URL: <http://dx.doi.org/10.1080/01496390902880057>

PLEASE SCROLL DOWN FOR ARTICLE

Full terms and conditions of use: <http://www.informaworld.com/terms-and-conditions-of-access.pdf>

This article may be used for research, teaching and private study purposes. Any substantial or systematic reproduction, re-distribution, re-selling, loan or sub-licensing, systematic supply or distribution in any form to anyone is expressly forbidden.

The publisher does not give any warranty express or implied or make any representation that the contents will be complete or accurate or up to date. The accuracy of any instructions, formulae and drug doses should be independently verified with primary sources. The publisher shall not be liable for any loss, actions, claims, proceedings, demand or costs or damages whatsoever or howsoever caused arising directly or indirectly in connection with or arising out of the use of this material.

Modeling of RO Flux Decline in Textile Wastewater Reclamation Plants Using Variable Fouling Index

Thirdpong Srisukphun,¹ Chart Chiemchaisri,² and Kazuo Yamamoto³

¹Department of Environmental Engineering, Faculty of Engineering,
Kasetsart University, Bangkok, Thailand

²Department of Environmental Engineering/National Center of Excellence
for Environmental and Hazardous Waste Management, Faculty of
Engineering, Kasetsart University, Bangkok, Thailand

³Environmental Science Center, The University of Tokyo, Hongo,
Bunkyo-ku, Tokyo, Japan

Abstract: This research proposes the model for estimation of flux decline using the concept of “variable fouling index.” The change in fouling index is induced by the accumulative foulant on the membrane and by the adhesion of the foulant on the membrane. The analysis of operating data of textile wastewater reclamation plants using the variable fouling index concept has shown that this model which was derived from short-term data of bench scale achieves a promising accuracy for the estimation of flux decline and increase of net driving pressure in a long-term operation of pilot-scale and full-scale system.

Keywords: Flux decline, modified fouling index, reverse osmosis, textile wastewater, variable fouling index

Received 6 May 2008; accepted 6 February 2009.

Address correspondence to Dr. Chart Chiemchaisri, Associate Professor, Department of Environmental Engineering/National Center of Excellence for Environmental and Hazardous Waste Management, Faculty of Engineering, Kasetsart University, Bangkok 10900, Thailand; Fax: 662-5790730. E-mail: fengccc@ku.ac.th

INTRODUCTION

Presently, fresh water shortage has become a serious concern all over the world. Reclamation of industrial wastewater is one of the potential solutions to this problem. Huge water consumption in the textile industry, where water consumption reaches approximately 0.2 to 0.5 m³/kg of the finished product (1), is an attractive target for installing wastewater reclamation facilities. Reverse osmosis (RO) membrane has been successfully applied to the reclamation of textile wastewater (2,3); nevertheless, RO faces a hindrance relating to the fouling issue. This problem has adversely affected plant performance both in terms of quantity and quality. It increases the operating cost due to an enlargement of overall resistance as reflected by increased a transmembrane pressure (TMP), routine-cleaning cycles, a corrosive by-product from the microorganism, and an increased salt passage (4,5,6,7).

In the past, many flux decline models have been proposed. These models can be explained excellently for the flux decline behavior of their equipment. However, applying bench-scale models to assess the membrane productivity on a larger scale was a predicament due to the different conditions between the bench-scale and the larger scale plants. The instances of this problem are membrane configurations, size of membrane elements, recovery ratio, operating conditions, i.e., constant flux and constant pressure, etc. Hence, development of the model for assessment of membrane productivity using least data and smallest experiment has been a challenging endeavor.

This research is proposing another simple and effective model for the assessment of flux decline in a longer operation time and larger-scale plant from short-term data of the bench-scale experiment. The operating data of bench-scale and pilot-scale from the textile wastewater reclamation plants were compared.

BACKGROUND

Review on Modeling of Membrane Flux Decline

RO process design was proposed by Pervov based on the evaluation of accumulative mass on membrane using a recirculation mode experiment (8). The accumulative mass was determined by measuring the change in concentration in wastewater.

The normalized fouling rate (NFR) was a model for estimating the flux decline and cleaning interval time in ultrafiltration (UF) based on the constant flux operation (9). The fouling rate of UF was assumed constant in this model.

The pore diffusion transport model was developed for the prediction and simulation of the permeate flux and concentration of permeate and concentrate by Tu et al. (10). The resistance due to membrane, concentration polarization, adsorption in membrane pores, and gel formation were included in this model.

Braeken et al. (11) proposed the prediction model of flux decline in NF due to adsorption of dissolved organic compounds. The adsorption thermodynamics were applied and the logarithmic function of the time was obtained for the fraction of the fouled membrane surface.

Theory

Generally, the classical superior equation, resistance in series of model (Equation 1), has been used to describe the relationship between the permeate flux and the membrane resistance (12). The reduction of permeate flux caused by the increase of foulant resistant (R_F) as shown in Eq. (2), which can be expressed in term of adsorption resistance (R_A), the pore blocking resistance (R_P), the cake filtration resistance (R_C), and the concentration polarization resistance (R_{CP}), over the resistance due to the membrane itself (R_M). In case of long-term operation, fouling plays an important role for change in the total hydraulic resistance. Hence, the permeate flux can be assessed if the total hydraulic resistance can be estimated.

$$J = \frac{\Delta P}{\eta(R_M + R_A + R_{CP} + R_P + R_C)} \quad (1)$$

$$J = \frac{\Delta P}{\eta(R_M + R_F)} \quad (2)$$

where R_F is a foulant resistance, which is defined as proportional to the specific volume containing the foulant (V/A , where V is the permeate volume and A is the membrane area) multiplied by the fouling index (I). Furthermore, R_F is also defined as a function of specific cake resistance (α) multiplied by the cake concentration (C) as shown in Eq. (3).

$$R_F = \frac{V}{A} I = \alpha C \quad (3)$$

Substituting the foulant resistance from Eq. (3) in Eq. (2), the permeate flux can be expressed as shown in Eq. (4).

$$J = \frac{\Delta P}{\eta[R_M + (\frac{V}{A} I)]} \quad (4)$$

Specific flux (L) or permeability is an important parameter which is useful for the operation with constant flux, a normal operation of RO system (9). The specific flux can be calculated from the ratio of permeate flux (J) and net driving pressure (ΔP) or can be calculated from the reverse product of total resistance (R_T) and dynamic viscosity (η) as shown in Eqs. (5) and (6). The net driving pressure was determined from the difference between applied pressure and osmotic pressure.

$$L = \frac{J}{\Delta P} = \frac{1}{\eta R_T} \quad (5)$$

$$L = \frac{1}{\eta [R_M + (\frac{V}{A} I)]} \quad (6)$$

MODELING OF FLUX DECLINE USING THE CONCEPT OF VARIABLE MEMBRANE FOULING INDEX

Generally, the fouling index is assumed to be a constant parameter and the permeate flux (J) is dependent upon the foulant resistant (R_F) and the permeate volume as defined in the theory of modified fouling index (MFI). MFI is determined from the gradient of the linear legon in the plot of t/V and V as presented in Eqs. (7) and (8) (13).

$$\frac{t}{V} = \frac{\eta R_M}{\Delta P A} + \frac{\eta I}{\Delta P A^2} V \quad (7)$$

$$MFI = \frac{\eta I}{\Delta P A^2} \quad (8)$$

According to the MFI concept, the specific flux (L) can be determined by the rearrangement of Eq. (6) as shown in Eq. (9).

$$\frac{1}{L} = \eta R_M + \eta I \frac{V}{A} \quad (9)$$

In the case of a spiral wound membrane filtration unit, the fouling rate or fouling index always decreases with filtration time because of a cross-flow velocity and a decrease of adhesion of foulant on membrane, hydrophobicity, hydrophilicity, and ionic strength. The cross-flow velocity limits the thickness of the foulant layer at the membrane surface by a detachment of the particle and a back diffusion of the solute (14). The hydrophobicity and hydrophilicity between the membrane and the foulant are changed when the membrane surfaces are occupied by the

foulant (15,16). The ionic strength between the membrane and the foulant are changed by Donnan equilibrium and this equilibrium prevents the diffusion of the ion between membrane and bulk solution (17).

In Eq. (6), when the dynamic viscosity and the resistance due to membrane are constant, specific flux is primarily influenced by specific volume (V/A) and fouling index (I). The specific volume is determined by multiplying the permeate flux and the filtration time. In addition, in this research, the fouling index is defined as a variable parameter. The variable fouling index is a function of an initial fouling index (I_o) and a reduction coefficient (δ). The n-order rate law is considered to estimate the model parameters as shown in Eq. (10).

$$\frac{dI}{d(V/A)} = -\delta I^n \quad (10)$$

The n-order rate law is integrated from $I = I_o$ to $I = I$ and $V/A = 0$ to $V/A = V/A$. The integrated rate law becomes:

$$\frac{1}{I^{(n-1)}} = \frac{1}{I_o^{(n-1)}} + (n-1)\delta \frac{V}{A} \quad (11)$$

According to the Eq. (10), the reduction coefficient (δ) is determined by a linear plot between $1/I^{(n-1)}$ and V/A . Consequently, Eqs. (6) and (11) are combined and the specific flux profile is determined by Eq. (12) as variable fouling index (VFI) model. The variable fouling index model is appropriate for both the constant flux operation and the constant pressure operation.

$$L = \frac{1}{\eta \left\langle R_M + \left[\frac{V}{A} \left\{ \frac{I_o^{(n-1)}}{1 + [(n-1)\delta \frac{V}{A} I_o^{(n-1)}]} \right\}^{\frac{1}{n-1}} \right] \right\rangle} \quad (12)$$

MATERIALS AND METHODS

This research studied the accuracy of flux decline model with variable fouling index using the different textile wastewater and the different treatment systems. The parameters of the model were determined from the flux decline data of bench-scale obtained from factory A (yarn and knit dyeing factory) and factory B (yarn printing factory). The models which were determined from the bench-scale experiments were compared with the operating data of pilot-scale experiment to test the competency in flux decline assessment of larger scale and longer operating time.

Pretreatment and RO Processes of Pilot-Scale Plants

Two textile wastewater treatment plants, Factory A and Factory B, had been chosen to represent the RO plants in this study. RO pretreatment for factory A was a membrane bioreactor (MBR). In addition, RO pretreatment for factory B was a combination of an activated sludge (AS) and a microfiltration (MF) membrane. The treated wastewater was further treated by RO unit at a feed flow rate of $0.4 \text{ m}^3/\text{h}$ and a permeate flow rate of $0.2 \text{ m}^3/\text{h}$. The system was operated under recirculation mode at a flow rate of $0.8 \text{ m}^3/\text{h}$. Two elements of a negatively charged membrane (model XLE-4040, Film Tech Corp.) with a diameter of 4 inches were occupied. The concentrate water from the first element was filtered again by the second RO element. The additive chemicals, biocide solution (Kuriverter EC 503, Kurita Water Industry LTD.), and anti-scalant solution (Kulifloat, Kurita Water Industry LTD.) were added continuously for controlling biofouling and scaling. Moreover, the pH value of the feed water was controlled to near 6.5. The RO unit was operated with a recovery ratio of 50%.

RO Feed-Water

The characteristics of treated wastewater which were obtained from MBR (Factory A) and MF (Factory B) are shown in Table 1.

Table 1. The characteristics of raw wastewater and treated wastewater

Parameter	Unit	MBR effluent ^a		MF effluent ^b	
		Range	Average	Range	Average
EC	$\mu\text{s}/\text{cm}$	3,580–5,150	4,343	2,570–5,510	3,224
SDI	–	1.87–4.54	3.55	0.95–5.28	2.3
pH	–	7.89–8.53	8.24	3.2–8.5	7.3
COD	mg/L	27.6–48.6	44	7.6–107	66
BOD ₅	mg/L	ND	ND	9.2–18.8	14.5
SS	mg/L	ND	ND	ND	ND
Color	mg/L as Pt-Co	43–273	138	30–67	45
TKN	mg/L	2.1–12.5	4.5	3.1–10.2	6.2
TP	mg/L	1.48–8.16	6.1	2.1–6.5	4.2

Note. ND was not detected.

^ais the treated textile wastewater from factory A.

^bis the treated textile wastewater factory B.

The treated wastewater was adjusted to a pH of approximately 6.5 to 7.0 using hydrochloric acid (HCl). They were generated for three types of feed-water i.e.

1. without chemical addition,
2. addition of anti-scalant (Kurifloat, Kurita Water Industry Ltd.) of 5 mg/L,
3. addition of anti-scalant 5 mg/L and biocide (Kuriverter EC 503, Kurita Water Industry Ltd.) of 5 mg/L as shown in Table 2.

The optimum anti-scalant and biocide doses were obtained from laboratory filtration experiment using actual wastewater.

Bench-Scale Set Up and Membrane Properties

The fouling in terms of flux decline was studied using a bench-scale experiment. A spiral-wound membrane filtration unit (Fig. 1) was employed in this study. The spiral-wound RO membrane with a negatively charged surface, and a diameter of 0.05 m. was fitted in the pressure vessel. The membrane filtration unit was operated at a feed flow rate of 0.027 L/s which is the minimum feed flow rate recommended by the membrane manufacturer, and a constant applied pressure of 0.35 MPa, respectively. The permeate flux profile was monitored for 30 days in one experiment.

The general properties of composite polyamide membrane, which was used in this part, were tested with 1,500 mg/L of NaCl feed solution, applied pressure of 1.5 MPa, and cross-flow velocity of 2.5 m/s. Average values of EC rejection, the initial specific flux, and the membrane resistance (R_m) were 96.22 %, 0.83 m/d-MPa, and $1.311 \times 10^{14} \text{ m}^{-1}$, respectively.

Table 2. The experimental conditions of bench-scale experiment

Experimental condition	Chemical addition
Factory A	
A1	without addition
A2	anti-scalant 5 mg/L
A3	anti-scalant 5 mg/L and biocide 5 mg/L
Factory B	
B1	without addition
B2	anti-scalant 5 mg/L
B3	anti-scalant 5 mg/L and biocide 5 mg/L

Note. RO feed-water was adjusted to a pH of around 6.5–7.0 using HCl.

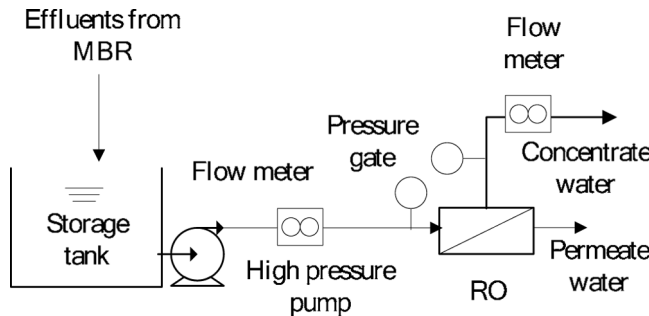


Figure 1. Schematic diagram of the spiral wound membrane filtration unit.

Estimation of Model Parameters

The model parameters were determined from three operating periods of bench-scale experiment i.e., 1 day, 7 days, and 30 days of operation. The specific flux (L_{model}), which was calculated from three sets of model parameters, was compared with the experimental data ($L_{experiment}$) to determine the appropriate operation period for the modeling. The sum of square error (SSE) as shown in Eq. (13) was used to evaluate the accuracy of the models. The operating period, which provided the smallest amount of difference in specific flux between model and experiment, the minimum SSE, was selected to be the optimum operation period.

$$SSE = \sum (L_{experiment} - L_{model})^2 \quad (13)$$

RESULTS AND DISCUSSIONS

Bench-Scale Experiment

The bench-scale experiments were conducted to determine the pattern of flux decline and the variation of fouling index. The experimental results are shown in Table 3. Under all cases, the specific flux and fouling index decreased rapidly within 1 day. In addition, after 7 days of experiment, the specific flux and fouling index decreased slightly until the end of experiment.

According to the results in Table 3, the addition of anti-scalant and biocide tended to increase the rejection efficiency in term of EC-rejection. Moreover, these additive chemicals lower the final fouling index and the final increased specific flux as noted from comparing between conditions A1 and A3 and conditions B1 and B3.

Table 3. The experimental results of bench-scale experiment

Data	Experimental conditions					
	A1	A2	A3	B1	B2	B3
Specific flux (m/d-MPa)						
L ₁ hour	0.771	0.829	0.961	0.943	1.021	0.935
L ₁ day	0.425	0.563	0.663	0.664	0.664	0.662
L ₇ days	0.447	0.538	0.553	0.411	0.540	0.629
L ₃₀ days	0.444	0.503	0.518	0.310	0.508	0.549
Fouling index (m ⁻²)						
I ₁ hour	5.62 × 10 ¹⁵	1.50 × 10 ¹⁶	7.89 × 10 ¹⁵	2.36 × 10 ¹⁵	2.09 × 10 ¹⁵	3.54 × 10 ¹⁵
I ₁ day	2.54 × 10 ¹⁵	1.80 × 10 ¹⁵	9.63 × 10 ¹⁴	5.32 × 10 ¹⁴	5.16 × 10 ¹⁴	4.79 × 10 ¹⁴
I ₇ days	5.51 × 10 ¹⁴	2.52 × 10 ¹⁴	2.41 × 10 ¹⁴	2.68 × 10 ¹⁴	1.23 × 10 ¹⁴	8.09 × 10 ¹³
I ₃₀ days	1.42 × 10 ¹⁴	1.01 × 10 ¹⁴	8.15 × 10 ¹³	1.29 × 10 ¹⁴	4.03 × 10 ¹³	3.04 × 10 ¹³
Average EC-rejection (over 30 days)						
EC _{feed} (µS/cm)	3,844 ± 340	3,986 ± 284	3,944 ± 150	2,968 ± 60	2,716 ± 131	2,690 ± 126
EC _{concentrate} (µS/cm)	3,917 ± 349	4,066 ± 290	4,030 ± 154	3,066 ± 106	2,834 ± 308	2,802 ± 100
EC _{permeate} (µS/cm)	156 ± 42	134 ± 16	118 ± 19	104 ± 49	90 ± 66	72 ± 12
Rejection (%)	95.97	96.67	97.04	96.55	96.76	97.37

Estimation of Model Parameters and Determination of Model Accuracy

The specific flux data of the bench-scale experiment from both factories were calculated for the fouling index parameters. Subsequently, three sets of fouling index data obtained from the different operation periods (1 day, 7 days, and 30 days) were plotted against the specific volume to determine three sets of the initial fouling index (I_o) and the reduction coefficient (δ). Consequently, the estimated specific flux profiles were calculated from these empirical parameters. The accuracies of these empirical parameters obtained from the different operating periods were compared.

In case of factory A, the model parameters and the calculated profiles of specific flux are shown in Table 4 and Fig. 2, respectively. It was found that the appreciating order of reaction rate is 2.2 for all conditions. Moreover, similar profiles were achieved from all of the models which were calculated from different operation periods. The values of SSE of condition A1 were 0.214, 0.149, and 0.132, for the operation periods of 1 day, 7 days, and 30 days, respectively. In addition, the SSE values of condition A2 were 0.133, 0.032, and 0.028. The values of SSE of condition A3 were 0.033, 0.032, and 0.012. From these results, the lowest SSE value was achieved from the operation period of 30 days. The model derived from condition A3, the normal operating condition of pilot-scale plant, which

Table 4. Comparison of model parameters between different periods from factory A

Parameters	Experimental condition		
	A1: without chemical addition	A2: addition of anti-scalant	A3: addition of anti-scalant and biocide
1 d			
I_o (m ⁻²)	3.561×10^{14}	1.117×10^{15}	6.011×10^{14}
δ (m ⁻¹)	2.155×10^{-17}	9.673×10^{-18}	1.421×10^{-17}
SSE	0.214	0.133	0.033
7 d			
I_o (m ⁻²)	2.895×10^{14}	1.118×10^{16}	7.735×10^{14}
δ (m ⁻¹)	2.155×10^{-17}	2.180×10^{-18}	1.755×10^{-17}
SSE	0.149	0.032	0.032
30 d			
I_o (m ⁻²)	6.480×10^{14}	1.193×10^{16}	5.147×10^{15}
δ (m ⁻¹)	1.789×10^{-17}	2.059×10^{-19}	1.811×10^{-17}
SSE	0.132	0.028	0.012

Note. $n = 2.2$.

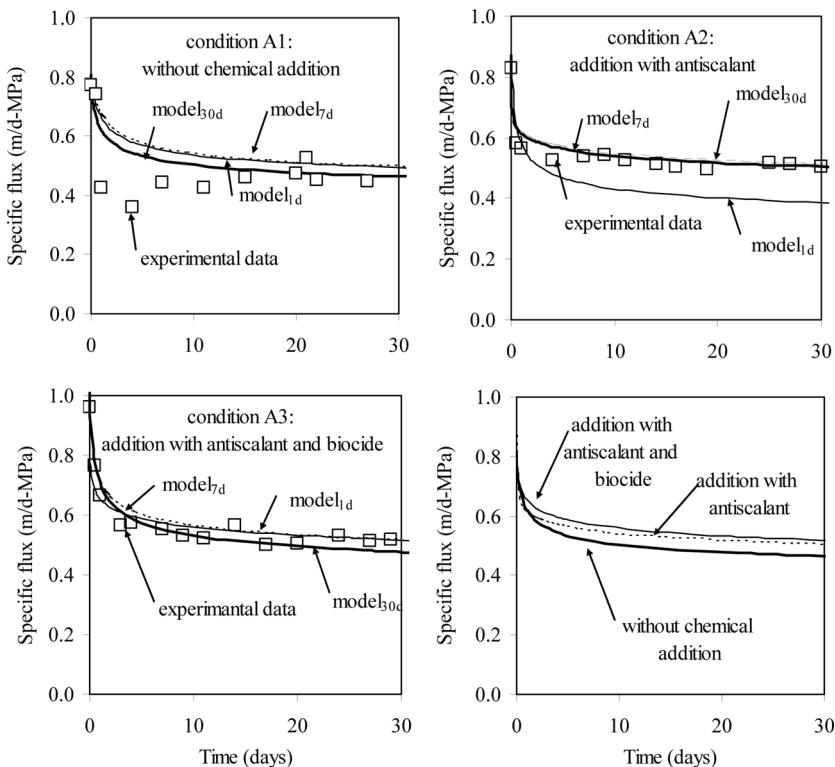


Figure 2. Comparison of the calculated specific flux profile between different operating periods (1 day, 7 days, and 30 days) using the data of factory A.

was calculated from the period of 30 days, is shown as follows:

$$L = \frac{1}{\eta \left\langle R_M + \left[\frac{V}{A} \left\{ \frac{(5.147 \times 10^{15})^{1.2}}{1 + [(1.2) \times 1.8110 \times 10^{-17} \frac{V}{A} (5.147 \times 10^{15})^{1.2}]} \right\}^{\left(\frac{1}{12}\right)} \right] \right\rangle} \quad (14)$$

In case of factory B, Table 5 and Fig. 3 shows the empirical parameters and the specific flux profiles of each experimental condition. The values of SSE of condition B1 were 0.242, 0.037, and 0.030 for the operation periods of 1 day, 7 days, and 30 days, respectively. In addition, SSE values of condition B2 were 0.183, 0.073, and 0.030. The values of SSE of condition B3 were 0.053, 0.051, and 0.029. From these results, the best fit was obtained from the model which was calculated from the period of 30 days, similar to factory A. The comparison of SSE values

Table 5. Comparison of model parameters between different periods from factory B

Parameter	Experimental case		
	Without chemical addition	Addition of anti-scalant	Addition of anti-scalant and biocide
1 d			
I_o (m ⁻²)	6.986×10^{14}	1.305×10^{14}	6.049×10^{14}
δ (m ⁻¹)	1.858×10^{-17}	2.067×10^{-17}	1.770×10^{-17}
SSE	0.242	0.183	0.053
7 d			
I_o (m ⁻²)	4.324×10^{14}	1.118×10^{16}	1.650×10^{14}
δ (m ⁻¹)	8.180×10^{-18}	1.910×10^{-17}	3.312×10^{-17}
SSE	0.037	0.073	0.051
30 d			
I_o (m ⁻²)	4.052×10^{14}	4.590×10^{14}	5.147×10^{15}
δ (m ⁻¹)	7.347×10^{-17}	1.832×10^{-17}	3.151×10^{-17}
SSE	0.030	0.035	0.029

Note. $n = 2.2$.

and specific flux between 1 day, 7 days, and 30 days operation suggested that the model, which was derived from the operation period of 7 days, is also in good agreement with the experimental data (Fig. 3). The model derived from condition B3 at 30 days operation period is showed in Eq. (15). From these results, it suggests that the bench scale operation data of 7 days or longer could be used for the estimation of empirical parameters for long term modeling of RO flux decline.

$$L = \frac{1}{\eta \left\langle R_M + \left[\frac{V}{A} \left\{ \frac{(5.147 \times 10^{15})^{1.2}}{1 + [(1.2) \times 1.301 \times 10^{-17} \frac{V}{A} (5.147 \times 10^{15})^{1.2}]} \right\}^{\left(\frac{1}{1.2}\right)} \right] \right\rangle} \quad (15)$$

Sensitivity Analysis of Model Parameters

Figure 4 shows the effect of reduction coefficient (δ), initial fouling index (I_o), and the rate-order (n). It was found that the change in reduction coefficient led to change in fouling index and specific flux profile. An increase in the reduction coefficient decreased the fouling index and led to an increase of the specific flux. On the other hand, the decrease in the reduction coefficient gave opposite results. The initial fouling index affected the specific flux only during the initial stage of operation.

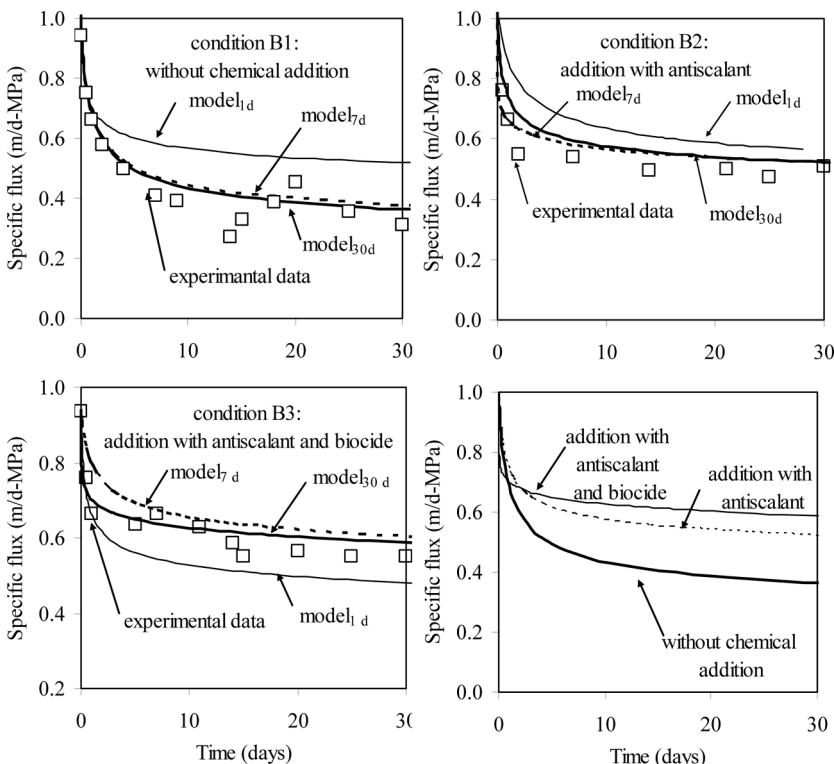


Figure 3. Comparison of the calculated specific flux profile between different operating periods (1 day, 7 days, and 30 days) using the data of factory B.

In long-term operation, the specific flux was not influenced by this parameter. The rate-order results in significant change of the specific flux profile. A minute increase of rate-order from 2.20 to 2.25 ($\sim +2.7\%$) yielded almost a constant profile of specific flux throughout the operation. In addition, a small decrease of rate-order from 2.20 to 2.15 ($\sim -2.7\%$) caused the large drop in the specific flux.

Model Competence in Assessment of Flux Decline in Larger Scale RO Units

The empirical parameters derived from both bench-scale reclamation plants, in which the anti-scalant and the biocide were added, were tested for their accuracy with long-term data of the pilot-scale plants. The specific flux profiles, which were determined from the model using constant fouling index concept (Eq. (9)) were also compared.

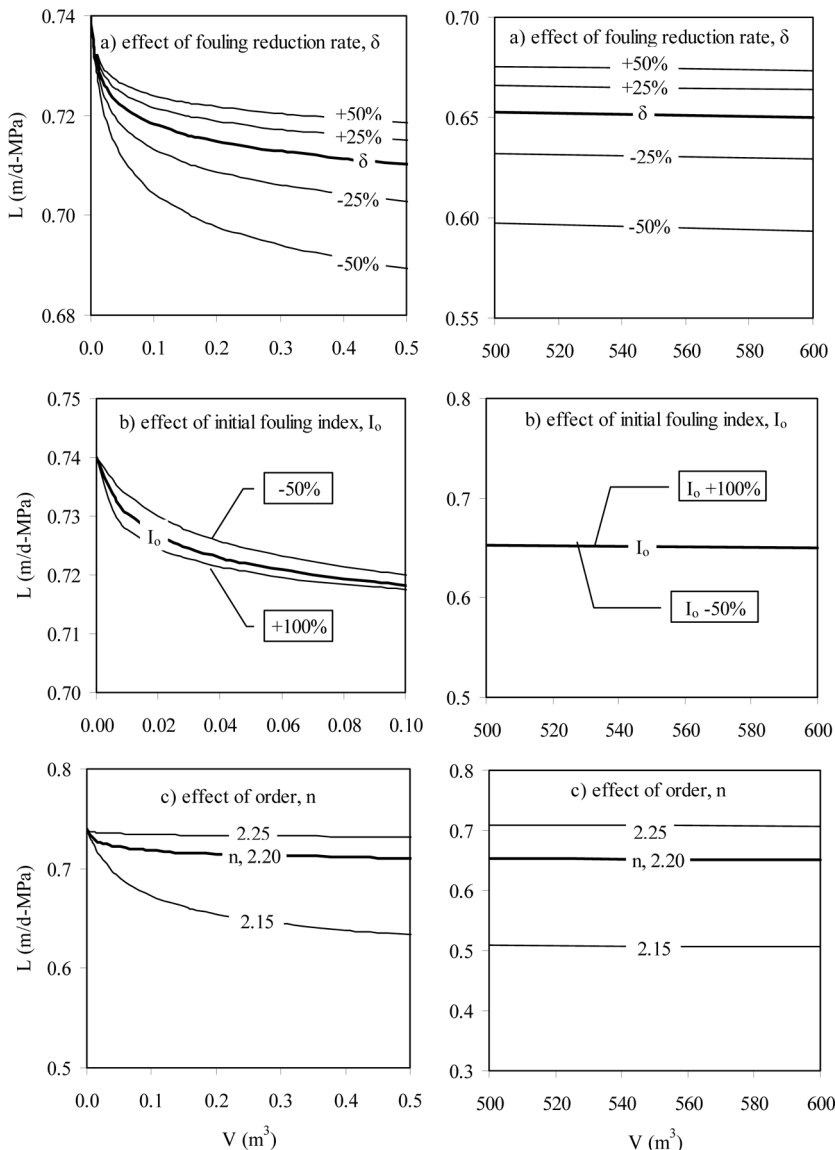


Figure 4. Model sensitivity analysis of wastewater from factory B.

Table 6 shows the empirical parameters comparing between constant fouling index model and variable fouling index model. Figure 5 shows the comparison of the specific flux and pressure profiles derived from

Table 6. The empirical parameters comparing between model with constant fouling index and model with variable fouling index

Parameters	Factory A	Factory B
Constant I		
$1/L_o = \eta R_M$	0.1998	0.1382
ηI	1.4976	1.3509
SSE	2.002	1.610
Variable I		
n	2.2	2.2
I_o	5.147×10^{15}	5.147×10^{15}
δ	1.811×10^{-17}	1.301×10^{-17}
SSE	1.379	1.340

Note. The models with constant fouling index were calculated from Eq. (8). The models with variable fouling index were calculated from Eq. (10).

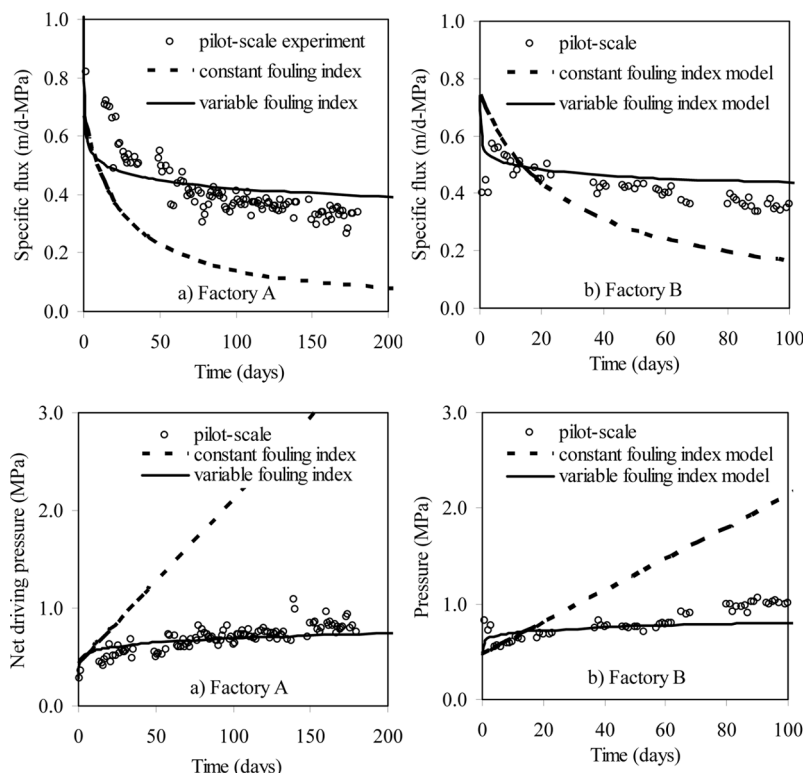


Figure 5. Comparison of the specific flux profiles and net driving pressure profiles between the constant fouling index model and the variable fouling index model.

constant fouling index and variable fouling index models with pilot scale operation data. In the comparison, the variable fouling index models of factory A and factory B previously described in Eqs. (14) and (15) are whereas the constant fouling index for factory A and factory B in Eqs. (16) and (17) are used.

$$\text{Factory A: } \frac{1}{L} = 0.1998 + 1.4976 \frac{V}{A} \quad (16)$$

$$\text{Factory B: } \frac{1}{L} = 0.1382 + 1.3509 \frac{V}{A} \quad (17)$$

It was found that, in case of Factory A, SSE values of the model with constant fouling index and a model of variable fouling index were 2.002 and 1.379 respectively. In case of Factory B, SSE values were 1.600 and 1.340. Hence, the model with the variable fouling index provided a more accurate estimation of specific flux and pressure in the RO system judging from the lower value of SSE.

CONCLUSIONS

This research is proposing a model for estimation of the specific flux profile in long-term operation of a full-scale plant using short-term data from the bench-scale experiment. The model with variable fouling index was developed for simulation of the RO unit. The results are summarized as follows:

1. The variable fouling index model was successfully used to model RO flux decline in a textile wastewater reclamation plant. It also provided more accurate results than the constant fouling index model.
2. In this study, bench scale operation data of 7 days or more provided a promising accuracy for the estimation of flux decline in long-term operation of larger scale system using variable fouling index model.
3. The membrane area and element size do not significantly affect the accuracy of the proposed model in this study. Short-term operation in a small-scale experimental set-up was successfully applied to assess the productivity of a larger plant in a long-term operation.

ACKNOWLEDGEMENT

The authors are grateful for the financial support given by Kasetsart University Research and Development Institute (KURDI).

NOMENCLATURE

A	membrane area (m^2)
C	cake concentration
I	fouling index (m^{-2})
I_o	initial fouling index (m^{-2})
J	permeate flux (m/d)
L	specific flux ($\text{m}/\text{d-MPa}$)
MFI	modified fouling index
n	order of reaction rate
R_A	adsorption resistance (m^{-1})
R_C	cake filtration resistance (m^{-1})
R_{CP}	concentration polarization resistance (m^{-1})
R_F	foulant resistance (m^{-1})
R_M	resistance due to membrane (m^{-1})
R_P	pore blocking resistance (m^{-1})
R_T	total resistance (m^{-1})
t	filtration time (day)
V	permeate volume (m^3)
ΔP	net driving pressure (MPa)
α	specific cake resistance
δ	reduction coefficient (m^{-1})
η	viscosity

REFERENCES

1. Marcucci, M.; Nosenzo, G.; Capanelli, G.; Ciabatti, I.; Corrieri, D.; Ciardelli, G. (2001) Treatment and reuse of textile effluents based on new ultrafiltration and other membrane technologies. *Desalination*, 138: 75.
2. Jiraratananon, R.; Sungpet, A.; Luangsowan, P. (2000) Performance evaluation of nanofiltration membranes for treatment of effluents containing reactive dye and salt. *Desalination*, 130: 177.
3. Suksaroj C.; Héran, M.; Allègre, C.; Persin, F. (2005) Treatment of textile plant effluent by nanofiltration and/or reverse osmosis for water reuse. *Desalination*, 178: 333.
4. Al-Ahmad, M.; Aleem, F.A.A.; Mutiri, A.; Ubaisy, A. (2000) Biofouling in RO membrane systems part1: Fundamentals and control. *Desalination*, 132: 173.
5. Baker, J.S.; Dudley, L.Y. (1998) Biofouling in membrane systems-A review. *Desalination*, 118: 81.
6. Brauns, E.; van Hoof, E.; Molenberghs, B.; Dotremont, C.; Doyen, W.; Leysen, R. (2002) A new method of measuring and presenting the membrane fouling potential. *Desalination*, 150: 31.

7. Chang, I.S.; Clech, P.L.; Jefferson, B.; Judd, S. (2002) Membrane fouling in membrane bioreactors for wastewater treatment. *J. Environ. Eng.*, *11*: 1018.
8. Pervov, A.G. (1999) A simplified RO process design base on understanding of fouling mechanisms. *Desalination*, *126*: 227.
9. Rabie, H.R.; Côté, P.; Adams, N. (2001) A method for assessing membrane fouling in pilot and full scale systems. *Desalination*, *141*: 237.
10. Tu, S.-C.; Ravindran, V.; Pirbazari, M. (2005) A pore diffusion transport model for forecasting the performance of membrane process. *J. Membrane Sci.*, *265*: 29.
11. Braeken, L.; van der Bruggen, B.; Vandecasteele, C. (2006) Flux decline in nanofiltration due to adsorption of dissolved organic compounds: Model prediction of time dependency. *J. Phys. Chem. B.*, *110*: 2957.
12. Schafer, A.L.; Fane, A.G.; Waite, T.D. (2005) Nanofiltration – Principles and Applications: Elesvier Advanced Technology, UK, p. 560.
13. Boerlage, Š.F.E.; Kennedy, M.D.; Aniye, M.P.; Abogrean, E. M.; E1-Hodali, D.E.Y.; Tarawneh, Z.S.; Schippers, J.C. (2000) Modified fouling indexultrafiltration to compare pretreatment processes of reverse osmosis feedwater. *Desalination*, *131*: 201.
14. Bian, R.; Yamamoto, K.; Watanabe, Y. (2000) The effect of shear rate on controlling the concentration polarization and membrane fouling. *Proc. of the Conference on Membranes in Drinking and Industrial Water Production*. L'Aquila, Italy. October 2000.
15. Wilbert, M.C.; Pellegrino, J.; Zydny, A. (1998) Bench-scale testing of surfactant-modified reverse osmosis/nanofiltration membranes. *Desalination*, *115*: 15.
16. Cornelis, G.; van der Bruggen, B.; Vandecasteele, C. (2005) Purification of surfactant containing effluents from the textile industry using ultrafiltration and nanofiltration. *Proc. of Membrane Process 2005. August, 21–26. Seoul, Korea*.
17. Thanuttamavong, M.; Yamamoto, K.; Oh, J.I.; Choo, K.H.; Choi, S.J. (2002) Rejection characteristics of organic and inorganic pollutants by ultra low-pressure nanofiltration of surface water for drinking water treatment. *Desalination*, *145*: 257.